Egyptian Journal of Geology, v. 62, 2018, p. 103-118

SEDIMENTOLOGY AND SEISMIC GEOMORPHOLOGY OF THE TIDAL-DOMINATED ESTUARINE INCISED VALLEY FILL: LATE MIOCENE QAWASIM RESERVOIR, ONSHORE EAST NILE DELTA

Abu Khadrah, A. M.[1], Selim S. S.[1], and Abdel Baset, A. A.[2]

1 Department of Geology, Faculty of Science, Cairo University, Giza, 12613 Egypt.
2 Wasco Oil Company, 5th Settlement, New Cairo,

ABSTRACT

The development of a tidal-dominated estuary above the Basal Messinian incision in the Lower Messinian Qawasim Formation in the onshore East Nile Delta province is interpreted from 3D seismic core, borehole images, and wireline logs data from four selected wells. Sedimentologically in terms of five facies associations of the Qawasim Formation are; tidally influenced fluvial channels, overbank muds, estuarine tidal channel, estuarine tidal bars and estuarine muds. These facies associations are building blocks for the depositional model that bounded by two incisions during the Early Messinain time. The lower cycle is called Qawasim level I which contains fluvial channel encased in overbank muds of fluvial plain. The upper cycle, Qawasim level II is characterized by estuarine tidal channel, estuarine tidal bars, and estuarine muds. The geomorphological characteristics of Qawasim Formation (lower and upper levels) can be detected using detailed seismic interpretations. The sedimentological and seismic characteristics of the Qawasim Formation in El Basant field may indicate the depositions in a tidal regime within estuary domain.

Keywords: Tidal-dominated estuary, seismic geomorphology, Qawasim Formation, Nile Delta, Egypt

INTRODUCTION

The importance of tidal deposits as hydrocarbon reservoirs have been recognized over the last decade in different parts of the world (e.g., Wightman and Pemberton, 1997; Marjanac and Steel, 1997; Martinius et al., 2001). The tidal deposits form some of the largest and most architecturally complicated hydrocarbon fields (Verdier et al., 1980; Carneiro de Castro, 1983; Marjanac & Steel, 1997; Higley, 1994; Ambrose et al., 1995; White et al., 1995; White and Barton, 1999; Martinius et al., 2000). Literature on tide-dominated or tide-influenced sedimentary systems, and generally on estuaries, is particularly vast. The most common classification of estuaries used by sedimentologists is that defined by Dalrymple et al., 1995. According to the prevailing hydrodynamics at the mouth of the estuary, waves or tidal currents, two end-members are distinguished, wave-dominated and tide-dominated estuaries. The Messinian incised valley fills of the Nile Delta province has a prolific gas producer for decades and still contains significant unexplored reserves (Dolson et al., 2002). They consist of stacked successions of fluvial, tidally influenced fluvial, bayhead delta and central basin mudstone facies (Dolson et al., op. cit.).

The main objectives of the present study are to investigate in detail the stratigraphic architecture, facies variability depositional environments, and evolution of the tidal-dominated estuary from the Qawasim Reservoir, East Nile Delta (Fig. 1). Including: 1) description and interpretation of the different lithologies and stratal geometries, precise correlation and integration of litho, bio-stratigraphical, and sedimentological data set to develop an understanding the depositional systems. 2) building-up a sequence stratigraphic scheme and achieving a better understanding of the depositional configuration of the Qawasim Formation through time and space. These are necessary to estimate the distribution and geometries of potential reservoirs.

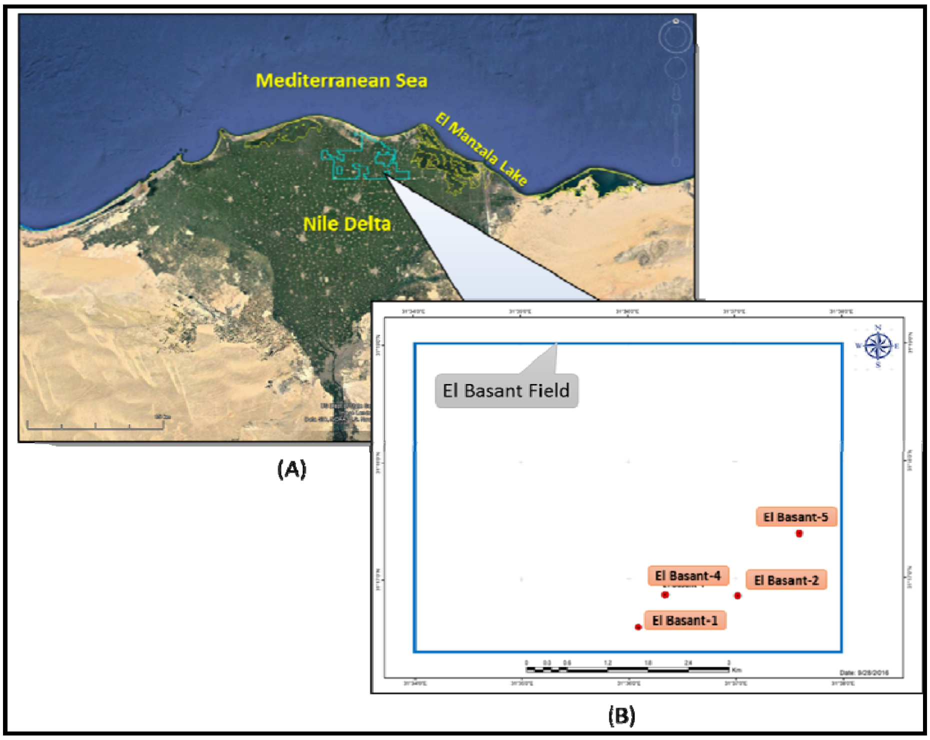

Fig. 1: a) index map of the Nile Delta, Egypt. b) location of El Basant development field, onshore East Nile Delta

GEOLOGIC SETTING AND STRATIGRAPHY

The database comes from the El Basant gas field located in the onshore part of the East Nile Delta, (Fig. 1). During the Messinian (7.24–5.33 Ma), the Mediterranean became progressively isolated from the Atlantic Ocean, triggering widespread precipitation of gypsum (5.96–5.6 Ma), massive salt deposition (5.6–5.5 Ma), and a dramatic sea level lowering followed by brackish water environments of "Lago-Mare" (Lake Sea) facies (e.g. Hilgen et al., 2007; Krijgsman and Meijer, 2008; Roveri et al., 2008). The sea level drop caused a large fall in Mediterranean water level followed by erosion and formation of large canyons incisions developed around the Mediterranean, as well as widespread deposition of salt in the basin depocenter (Dolson et al., 2005). The Mediterranean's Messinian salinity crisis triggered development of 5 major paleo-drainage systems along the northern Egyptian coastline (Dolson et al., 2002). The major canyons were filled with Qawasim and Abu Madi Formations deposits (Dolson et al., 2002; Pigott and Abdel-Fattah, 2014). The interval of interest is the Lower Messinian Qawasim Formation that occurs approximately 2500–3100 meters below the surface. The type section of Qawasim Formation is the Qawasim-1 well (onshore central delta), where it attains a thickness of 933 m. It has been described as a succession of thick sandy and conglomeratic beds. The formation comprises sandstones, siltstones and claystones; with some interbedded conglomerates of Tortonian to Messinian age of relatively marine conditions (EGPC, 1994). The stratigraphic relationship between the underlaying Sidi Salem and Qawasim formations is controversial. They are lateral facies equivalents (Abdel Aal et al., 1994) or are considered as separate Upper Miocene units (EGPC, 1994). The clastics of Qawasim Formation were sourced from the Lower Cretaceous Nubian sandstone and basement rocks in the southeast (EGPC, 1994). In the study area, the Lower Messinian Qawasim Formation is unconformably overlies and underlies the Sidi Salem and Abu Madi formations, respectively (Figs. 2 to 4).

Biostratigraphically, the Messinian succession is mainly lacks marine foraminifers except *Ammonia beccarii* and *Ostracods* (Rio et al., 1990) at some horizons (Fig. 5). On the other hand, the Messinian sequence is subdivided into Qawasim and Abu Madi formations being correlated with the two main nannoplanktonic zones; *Helicosphaera orientalis* (NN11b) *and Reticulofenestra rotaria* (NN11c), respectively (Rio et al., op. cit).

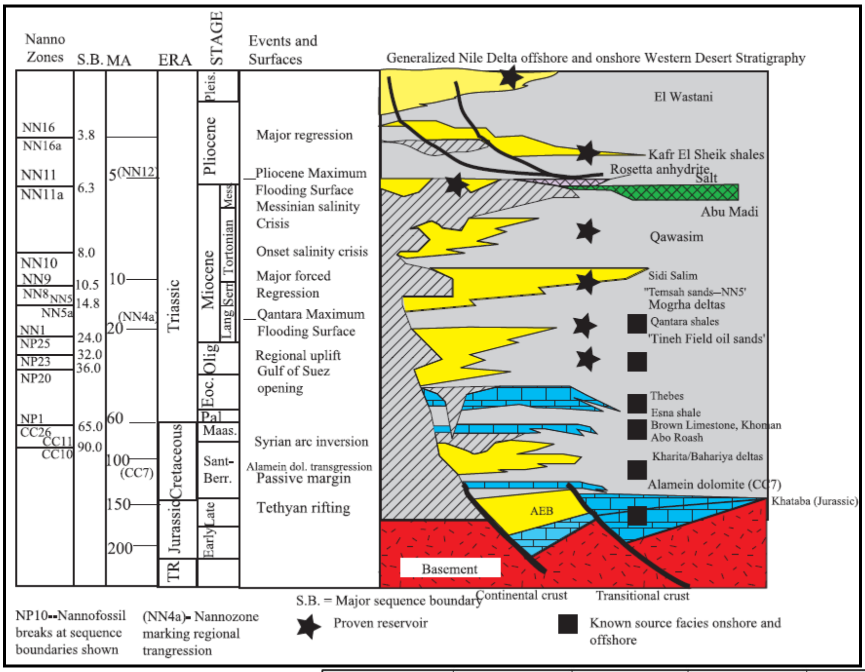

Fig. 2: Nile Delta tctono–stratigraphic column. The diagram represents onshore to offshore stratigraphy from the Western Desert to the deep water Nile Delta. Nannofossil assemblages shown are at key flooding surfaces and unconformities. (after Dolson et al., 2005)

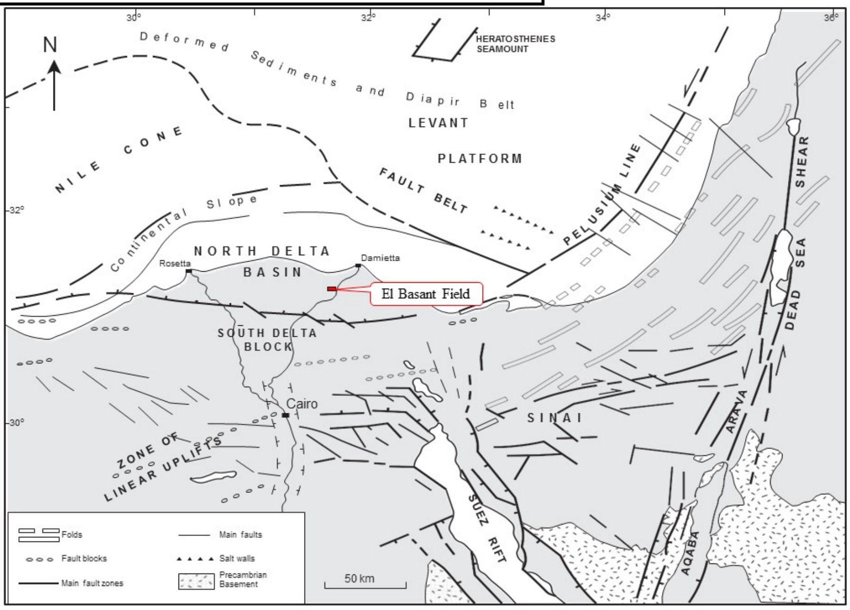

Fig. 3: Main tectonic features of the Nile Delta, Sinai and southeast Mediterranean region (after Sestini, 1989).

The Messinian deposits are transgressed by the marine flooding of the Pliocene (5.3 my) based on isotopic stratigraphy (Montanari et al., 1997). The Pliocene transgression is considered to be a consequence of the re-establishment of communications with the open sea (Ruggieri and Sprovieri, 1976).

The Nile Delta region experienced rifting and extension in the Jurassic and Early Cretaceous with development of east-west trending basins (Mosconi et al., 1996 and Loutit et al., 2001). This was followed by general thermal sagging and subsidence with shelf margin formation (Dolson et al., 2001). During the Late Cretaceous-Miocene, the Jurassic-Early Cretaceous rift basins were inverted with the development of Syrian arc series of large northeast-southwest oriented folds south of the Nile Delta and Eastern Mediterranean regions (Moustafa and Khalil, 1989, 1990, 1994; Shahar, 1994; Ayyad and Darwish, 1996; Abd El-Motaal and Kusky, 2003; Abd-Allah, 2008). The tectono-stratigraphic evolution of the east Nile Delta is shown in Fig. 2. The “hingeline” (Figs. 3 and 4) is an Upper Cretaceous carbonate shelf edge that forms the southern boundary of thick Neogene sediments in the Nile Delta. It is an important feature affected the overall stratigraphic and tectonic evolution of the Nile Delta basins (Said, 1981; Orwig, 1982; Harms and Wray, 1990). A subsequent rifting phase (Gulf of Suez rift) occurred during Oligo-Miocene with a dominant extension orientated in northwest faults due to divergence of the African plate away from the Arabian plate (e.g. Bosworth, 1994; Patton et al., 1994). The Oligo-Miocene or older E-W and NW trending faults in the Nile Delta were suggested to be related to the initial rifting phases of the Gulf of Suez (Abd-Allah et al., 2012; Hussein and Abd-Allah, 2001) (Fig. 3).

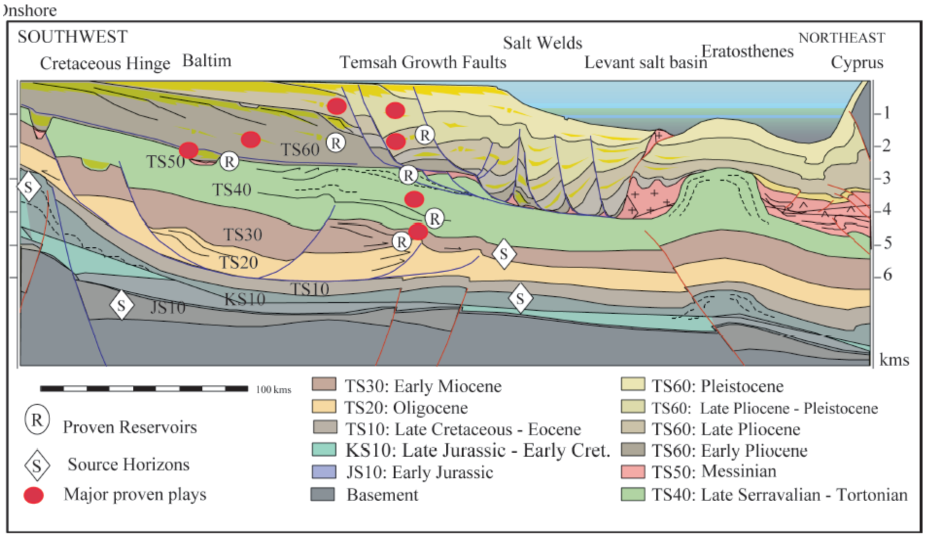

Fig. 4: Schematic diagram of Nile Delta stratigraphy and structure. Modified from Dolson et al. (2001); Dolson et al. (2000). Deep source rocks generate hydrocarbons which have migrated as high as the Pleistocene in some fields. Biogenic gas is also common in the shallower section. (Dolson et al., 2005).

The gross seismic stratigraphic framework of the study area is described with reference to main representative seismic section, perpendicular to the depositional direction of the Messinian depositional system (Fig. 4) and summarized in the stratigraphic chart (Fig. 2).

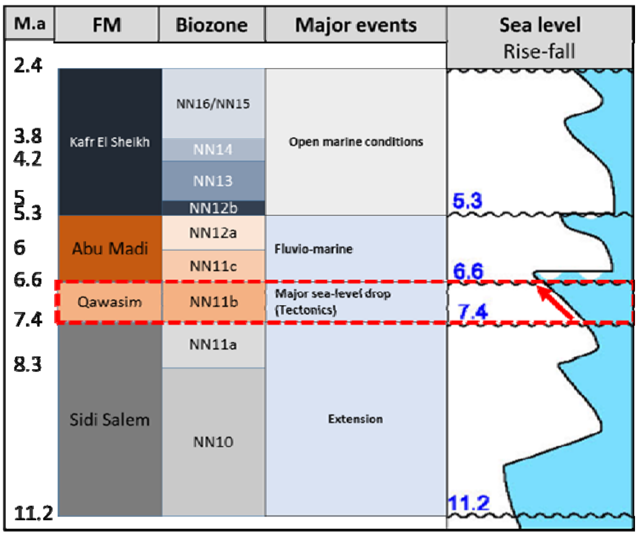

Fig. 5: Biostratigraphic chart and sea level cyclicity (EREX, 2012 modified after Rio et. al., 1990) shows the NN11b Zone of Qawasim Formation (7.4-6.6Ma).

Generally, The Qawasim Formation in El Basant area is located in a part of a large estuarine domain has NW-SE propagation direction, deposited during the back filling of the incised valley formed during Tortonian-Serravallian time, divided into three phases of filling; braided channels, meandered tidally influenced channels and tidal estuarine channels and bar system (WASCO IR, 2016). This formation is characterized by its chaotic nature on the seismic section (Fig. 7) being deposited in the lower part of the incised valley fill during the Early Messinian time (Figs. 7 and 8). It overlies Sidi Salem Formation and unconformably overlies by Abu Madi Formation of the Late Messinian age (Figs. 7 and 8).

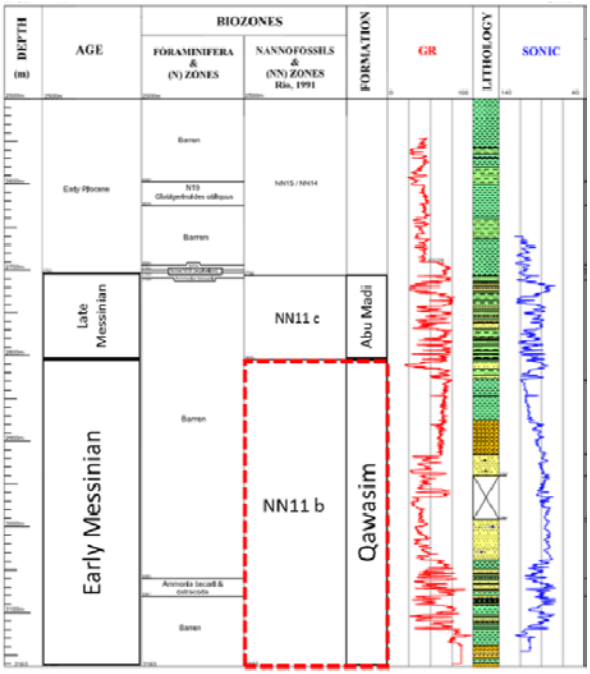

Fig. 6: Biostratigraphic summary chart of El Basant-1 well.

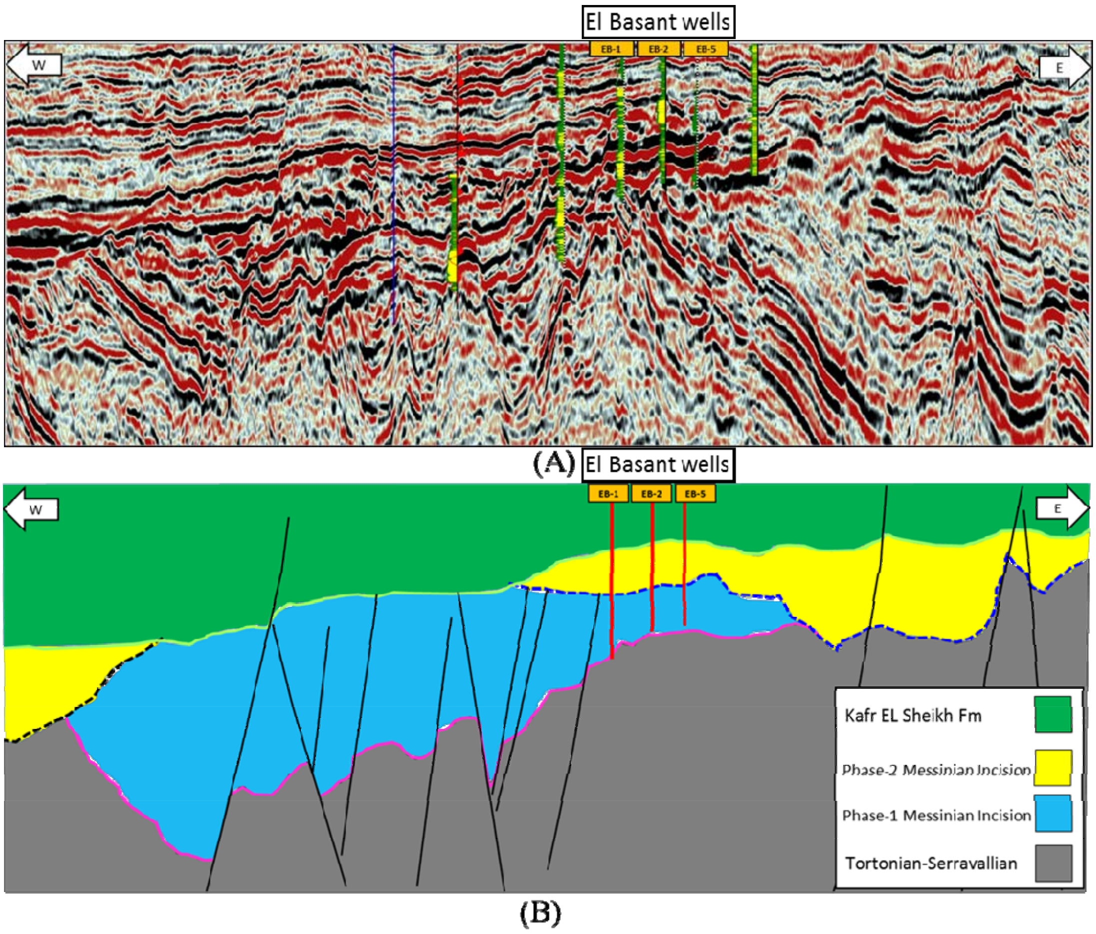

Fig. 7: A) Regional seismic line passing through El Dana Gas and El Wastani petroleum company concession without interpretation, (B) Diagrammatic fill of the regional seismic line showing the multi incisions during the Messinian time.

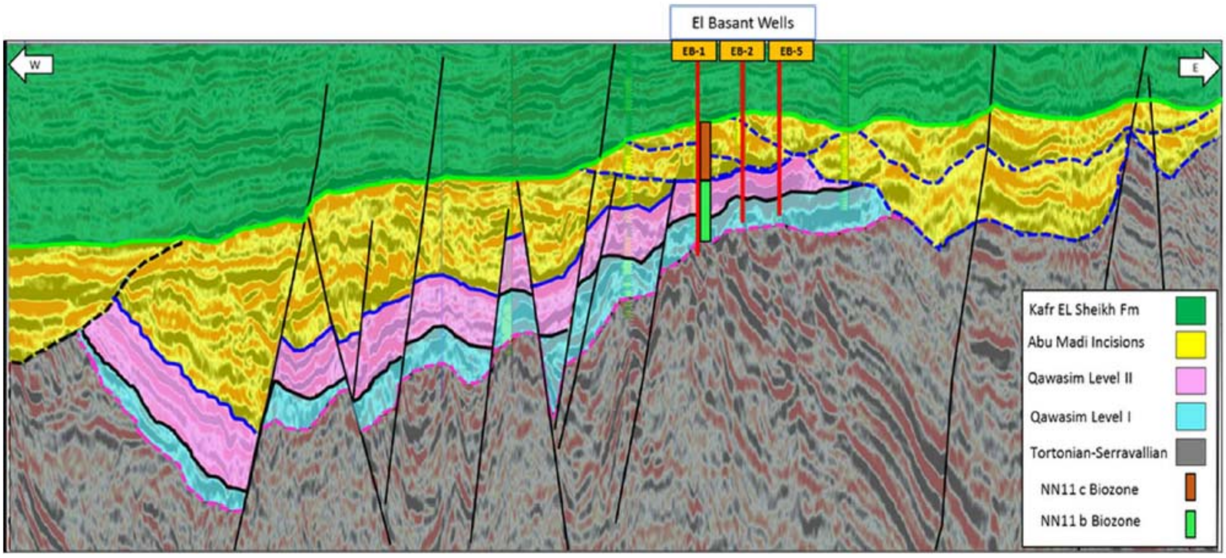

Fig. 8: Regional seismic line passing through the study area with the interpretation covering all the area shows the multi incision filling scenario of the Messinian age**.**

METHODOLOGY AND DATA SET

This study utilizes a comprehensive approach that integrates seismic interpretation, wireline log analysis, bore hole image and core of Upper Miocene Qawasim Formation in El Basant field. The methodology divided into four steps as follow:

A) **Biostratigraphic analysis:** biostratigraphic analysis of El Basant-1 well helps to delineate the Qawasim Formation sequence from Abu Madi Formation sequence. the Messinian is subdivided into two sequences Qawasim sequences and Abu Madi which mainly correlated with the two main nannoplanktonic zones; Helicosphaera orientalis (NN11b) and Reticulofenestra rotaria (NN11c), respectively (Figs. 5 and 6) (EREX, 2008).

B) **Seismic Interpretation:** a suite of 3D seismic lines (1700km^2 area) fully cover El Basant field. the detailed seismic interpretation focused on the horizon interpretations which may reflect the Lower Messinian general geomorphology. The seismic character helps to divide the Qawasim Formation into two levels (Qawasim level I and Qawasim level II) depending on hard kick on the seismic character (Figs. 7 and 8). The horizons seismic amplitude extraction is a suitable tool reflects the lateral distribution of the Qawasim Formation. Due to the limited resolution of the seismic data it's very important to integrate the seismic amplitude with the lithofacies and facies association resulted from the next two steps. This integration will check if some trends or geological features related could be provided from the seismic data to represent the depositional architecture related to regional overview of the big estuary.

C) **Core description:** 39.5m length core in El Basant-1 well represents the upper part of Qawasim Formation (Qawasim Level II) resulted into six lithofacies includes; parallel-laminated sandstone (Sl), Cross-laminated sandstone (Sxl), massive sandstone (Sm), heterolithics (HI), laminated mudstone (Ml), massive mudstone (Mm) (Table1). The core description allows sufficient resolution to recognize the different lithofacies and depositional elements within the Qawasim Level II. While the Qawasim Level I covered with BHI and wire-line logs only, so the distribution will be less accurate in comparable to the Qawasim level II that covered with all types of data.

D) **Wire-line logs and bore hole image analysis Interpretation:** The wire-line logs specially the gamma ray logs give a hints on the cyclicity and boundaries between the depositional units and allow to understand the lateral variation of facies between the wells of the study area. The correlation and integrations of the resulted lithofacies and depositional units from the core interpretations used to calibrate the e-facies produced from the bore hole image interpretation. The integration of the BHI and wire-line logs creates the corner stone input in the neural network technique. This technique helps to create a mathematical relation between the interpretation results from complete well data sets to the other wells. Finally, the neural network analysis technique creates the facies in the un-cored intervals of El Basant-1 wells and creates the facies in the other wells that contain only the wire line logs.

Table-1: Shows the Lithofacies description and interpretation with a snap shot from core and bore hole image from El Basant-1 well

Lithofacies	Description	BHI / Core photos
Cross-laminated Sandstone (Sxl)	consists of fine to medium grained unfossiliferous sandstone, characterizing by very low angle cross laminating sedimentary structure that could be a part of a large scale trough cross lamination. The color varied between grey to light grey with calcareous cement. Stratification was characterized by subtle changes in grain size and by very thin carbonaceous and/or muddy lamina (Mud drapes) may forms a double mud drapes in parts. The thickness of the cross lamination was set generally in millimeter scale.	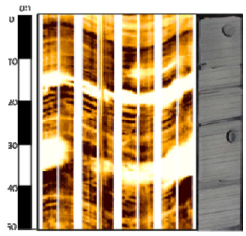
Parallel-laminated Sandstone (Sl)	consists of grey to light grey color, fine to medium grained and moderately sorted unfossiliferous sandstone. This facies is characterized by horizontal stratification. The stratification is characterized by subtle changes in grain size and by very thin carbonaceous and/or muddy laminae (Mud drapes) and may forms a double mud drapes in parts, with a gradational top and base. The individual laminae varied in thickness from millimeters to centimeters scales.	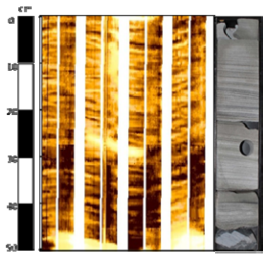
Heterolithics (Hl)	It consists of a succession of variable grain size deposits ranging from very fine to fine grain unfossiliferous sandstone. This lithofacies interbedded with mudstone and siltstone layers ranging from 5mm to 2cm thickness with wavy and lenticular lamination structure. Its color ranged from light grey to gray depending on the percentage of the muddy and silty layers in the intervals. This lithofacies had a gradational top and base.	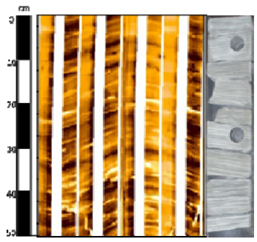
Laminated Mudstone (Ml)	It consists of grey-to dark grey laminated claystone and siltstone. Some local deformation and convoluted lamination are also described. Generally, its top and base is sharp. This lithofacies is characterized by presence of trace amount of Ammonia Beccaria and Ostracod as shown in the biostratigraphy of El Basant-1 well.	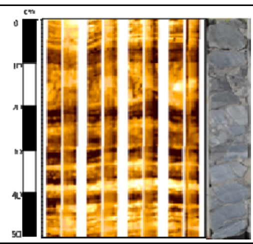
Massive Mudstone (Mm)	It consists of massive or structureless claystone and siltstone. It is grey to dark grey in color exhibiting some local deformation like convoluted lamination in parts, with sharp top and base in general. This lithofacies is characterized by rare occurrence of Ammonia beccarii and Ostracoda as shown in the biostratigraphy of El Basant-1 well	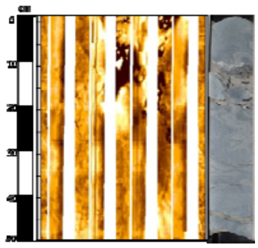

RESULTS

Conventional Core and borehole-image (BHI) sedimentary facies

Six lithofacies are recognized within the Qawasim Formation (Table 1). These lithofacies are identified based on the core-BHI-Log integration. The borehole image facies are calibrated with the corresponding cored interval in order to correctly recognize the sedimentary structures that are seen in the BHI images (e.g. Donselaar & Schmidt, 2005).

This step reduces the uncertainty in the interpretation of the sedimentary features. Therefore, a system of descriptive, simple and robust image facies was established based on identification of the following internal sedimentary structures: horizontal lamination, low-angle lamination, cross-stratification, mottling and deformed stratification. The lithological classes from the BHI were combined with Gamma Ray, Neutron/Density logs and accordingly the sedimentary facies are grouped into five facies associations (FA); tidally influenced-fluvial channel, overbanks deposits, estuarine tidal channels estuarine tidal bars, and estuarine mud.

Facies associations

Facies association 1: Tidally influenced-fluvial channel

<u>Description:</u> This facies association is composed mainly of massive sandstone (Sm) lithofacies with subordinate cross-laminated sandstone (Sxl) lithofacies, it shows a serrated fining upward, while in some parts shows clear coarsening on gamma ray patterns (Fig. 9). This association is characterized by porosity ranges from 10% to 28% (Fig. 10). It acts as a target reservoir within the Qawasim level I. Its thickness varies from 5m to 30m (Fig. 9). It is bounded by an erosive base and top with internal deformation and re-activation surfaces on the bore hole image (Fig. 11). Laterally, this association was intercalated with the overbanks muddy facies in all directions.

<u>Interpretation:</u> This facies association was deposited during Qawasim level I above the base Messinian unconformity during the major sea level fall at 7.4Ma (Rio, et al., 1990). It was deposited under a waning flow regime typical of channel prone (Smith, 1988). The fluvial deposits were confirmed by moderate to high sinuosity fluvial channel on the extracted (maximum negative) amplitude from El Basant field seismic volume (Fig. 10). The coarsening upward pattern of the gamma ray may be related to the deposition of crevasses splay units within this assembly as shown in El Basant-5 well (Fig. 9). The massive sandstone facies lies over a scoured surface appearing in the bore hole image that might be deposited during a high energy condition within a fluvial channel deposits (Turner, 1974). This association is interpreted as a tidally influenced fluvial channel complex deposits.

Facies association 2: Overbanks

<u>Description:</u> It is composed of massive mudstone (Mm) lithofacies with minor amounts of laminated mudstone (Ml) lithofacies. Generally, this association is characterized by fine grained nature and intercalation of minor amounts of siltstone and very-fine sandstone. It shows irregular and serrated pattern on gamma ray log (Fig. 9). The bore hole image interpretation revealed some deformational texture like deformed lamination and bioturbations, while in some parts, it shows faint parallel lamination (Fig. 11). Its thickness was variable ranging from 3m to 15m, forming about 60% of the Qawasim level I thickness. Laterally, it is eroded or incised with the tidally influenced fluvial channels. This association may cause a lateral and stratigraphic sealing of the reservoir within Qawasim level I in El Basant field (Figs. 9 and 10).

<u>Interpretation:</u> Mud is the dominant deposits of these associations.

The rate of sedimentation was generally very slow which may have been deposited during a flood (Reineck & Singh, 1980). The serrated attitude of the gamma ray pattern shows the alternation between the silty and muddy staff deposits. This pattern might suggest the discharge rate fluctuation during the floodplain deposition mechanism (Reineck & Singh, op. cit.). In conclusion, this association was interpreted as an overbank deposits.

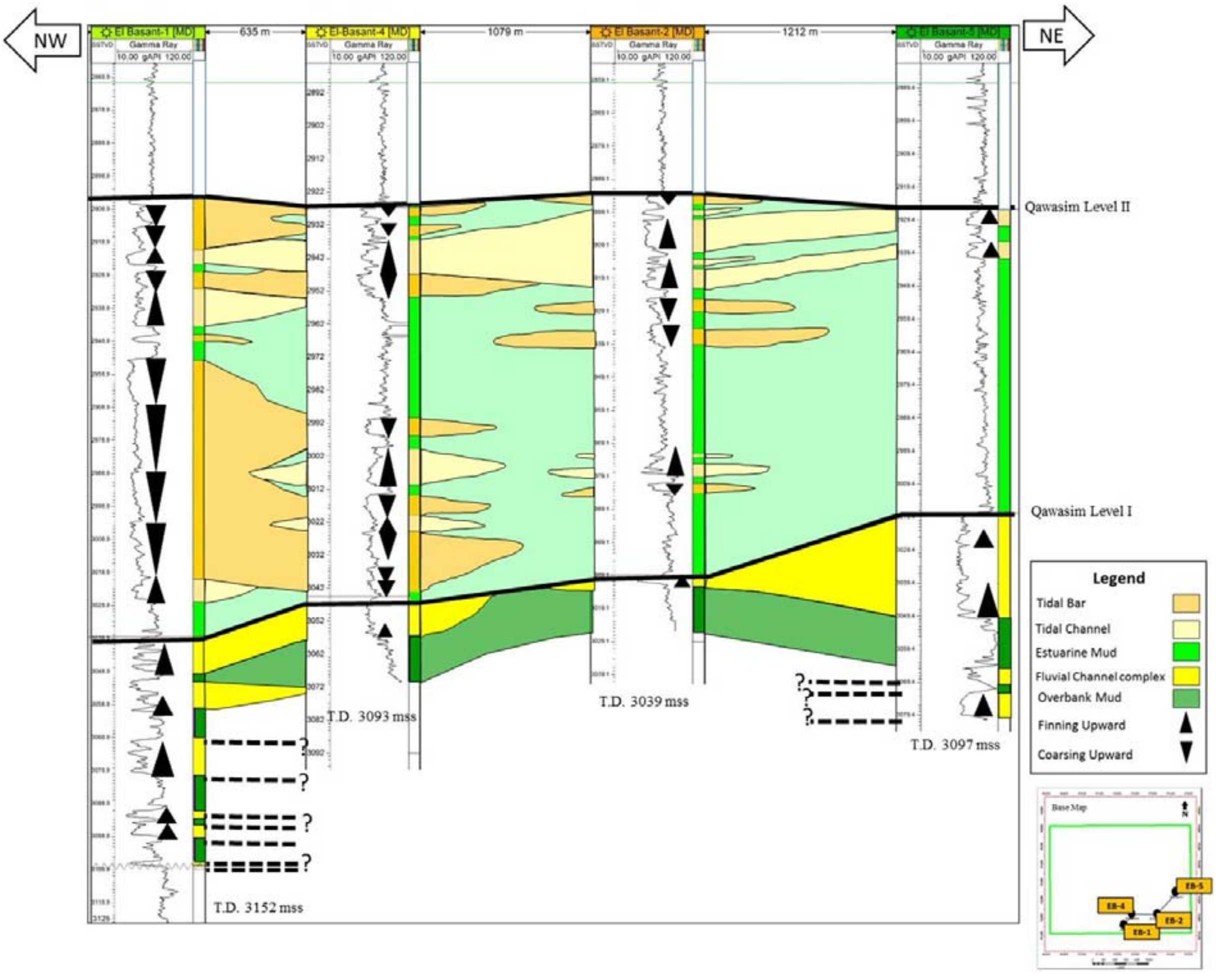

Fig. 9: Correlation panel between El Basant wells showing the lateral and vertical distribution of the facies association with the Gamma ray patterns.

Facies association 3: Tidal channels:

Description: This association comprises cross-laminated sandstone (Sxl) and massive sandstone (Sm) lithofacies. It shows a remarkable fining upward pattern on gamma ray log with a porosity ranging from 10% to 25% (Figs. 9 and 10). It is bounded at the base by either flat or erosive surface. It exhibits multi scour surfaces in some intervals appearing in the bore hole image of El Basant-1 well (Fig. 11). It forms a lenticular body of about 3m in thickness in parts. The internal structure of this association shows cross-lamination between 18° and 20° (Fig. 11). This association acts as a target reservoir within Qawasim level II. Its thickness is variable between 5m and 12m (Fig. 9). Laterally, this association cut into the estuarine mud in El Basant wells (Fig. 9).

Interpretation: The finning upward pattern sedimentary structures and lithofacies of this association may attest the deposition during a waning flow regime in tidal-dominated channel. Also, are conditions being typically of channel prone to lateral accretion (Smith, 1988). The presence of massive sandstone lithofacies may be related to the extensive bioturbation (Miall, 1996). The presence of the single and double mud drapes indicates the tidal regime deposition (Miall, op. cit.).

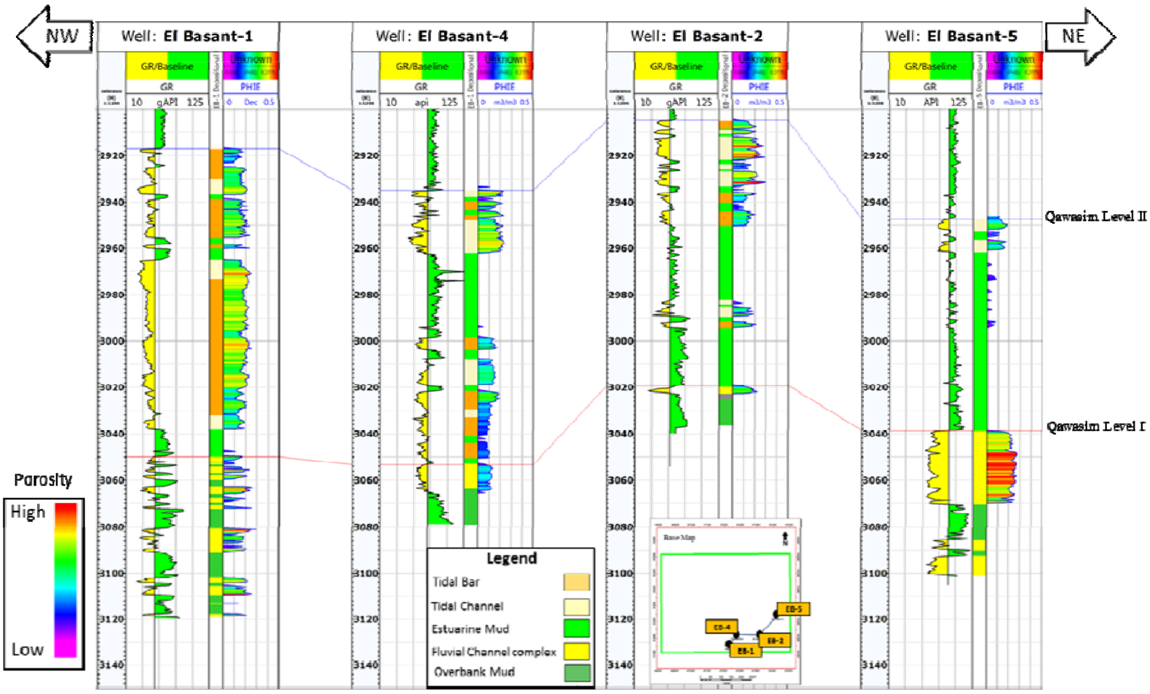

Fig. 10: Correlation panel between El Basant wells showing the effective porosity (PHIE) distribution of the facies association

Facies association 4: Tidal bars.

Description: This association comprises cross-laminated sandstone (Sxl) and parallel laminated sandstone (Sl) with subordinate massive sandstone (Sm) lithofacies. It shows a remarkable coarsening upward and blocky gamma ray log pattern with a distinctive fair porosity ranging from 11% to 19% (Figs. 9 and 10). It is bounded at the base by either flat or scouring surface. This association forms a lenticular body of 2m in thickness. Its internal structure showed planner lamination to very low angle cross-lamination ranging from 10° to 12°. The dip increases at the bottom of this association till it reached to 26° in some parts (Fig. 11). Hence, it acts as the main reservoir unit within Qawasim level II in two wells of the study area (El Basant-1and El Basant-4 wells). The thickness of this association is variable ranging from 2m to 64m and its maximum thickness presented in El Basant-1 well. It decreases away to the East and West directions from El Basant-1 well (Fig. 9).

Interpretation: The prevalence of laminated and cross laminated sandstone internally displayed planar to very low angle dipping stratification indicates that these sediments were deposited in the upper flow regime condition (Reineck & Singh, 1980). The coarsening upward pattern on the gamma ray log indicates that this unit might be a bar system (Reineck & Singh, op. cit.). The abundance of the mud drapes in this facies association indicates the fluctuation nature of flow during deposition (Miall, 1985, 1996). On the other hand, the fluctuation between the parallel- lamination and cross-lamination sedimentary structure revealed the fluctuation attitude of the system from upper to lower flow regime. These fluctuation phenomena might be applied to the tidal regime nature. This association was considered to be an estuarine tidal bar unit.

Facies association 5: Estuarine mud

Description: This association is composed mainly of laminated mudstone (Ml), massive mudstone (Mm) and Heterolithics (HI) lithofacies. The unit exhibits both sharp and gradational base and top (Fig. 11). Its thickness is variable and reach more than 80m. The highest appearance percentage of this association has been found in El Basant-5 well (Fig. 9). It is characterized by local deformations (Fig. 11).

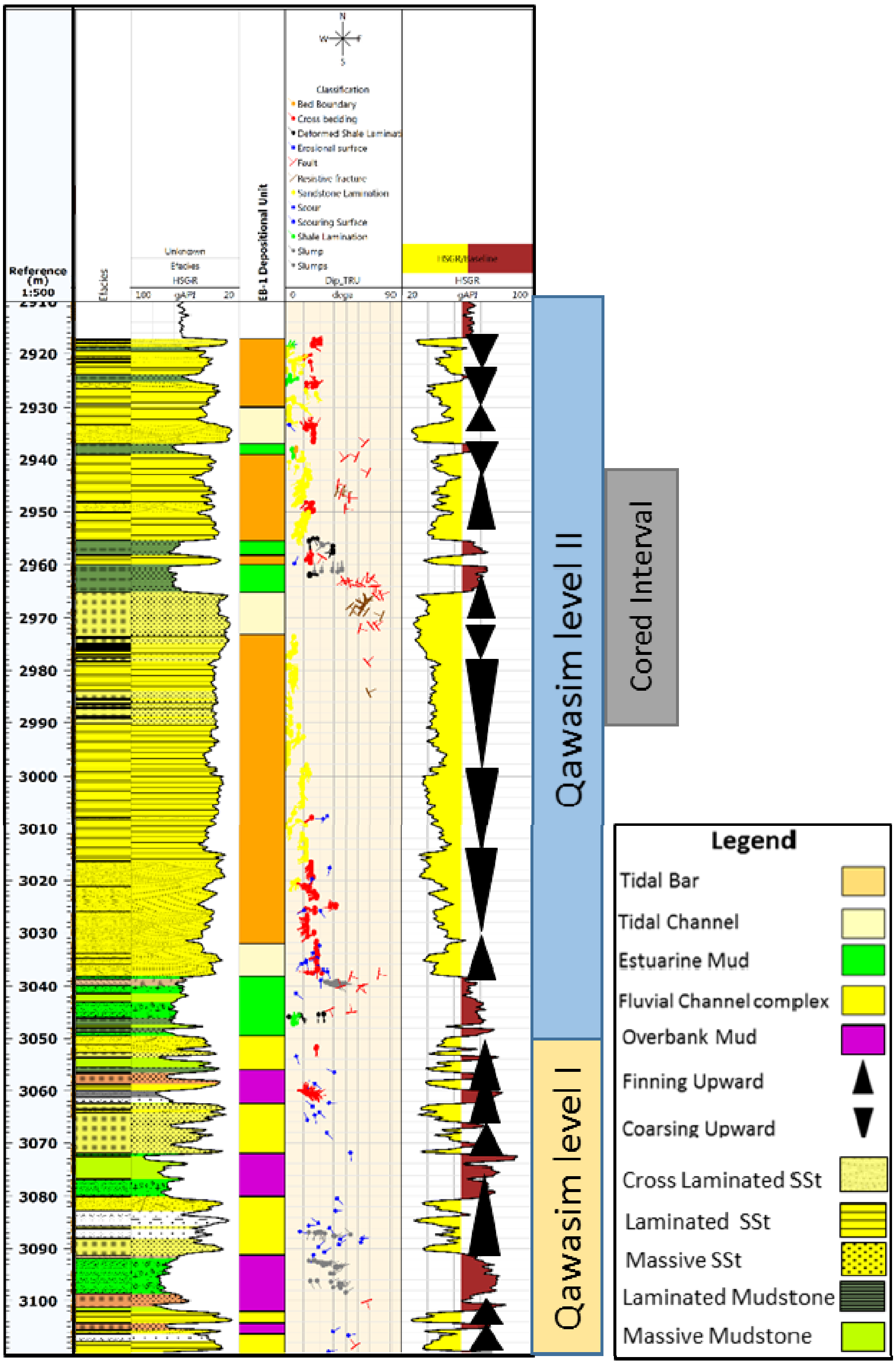

Fig. 11: Correlation panel between El Basant wells showing the effective porosity (PHIE) distribution of the facies association

<u>Interpretation:</u> The dominance of the massive and laminated mudstone lithofacies indicates suspension fallout under calm conditions (Uba et. al, 2005). On the other hand, the dark color of this facies might reveal anaerobic environment conditions (Nichols, 2009). The deformation of the laminae might be due to differential loading (Miall, 1985, 1996). The bore hole image interpretation of El Basant-1 well indicates that the local deformation of this association may be due to the micro-faults and/or extensive bioturbation activity (Fig. 11). The flaser laminations, wavy laminations and the alternation between the fine grained sandstone and mudstone might indicate the deposition from suspension settling to low flow regime (Miall, 1996). The silty layers represent traction deposition from ebb and flood tides whereas the clay layers represent the deposition from suspension during slack-water periods (Nichols, 2009). So that this unit was interpreted as an estuarine tidal mud.

DEPOSITIONAL MODEL AND DISCUSSION

The Messinian deep incision into the underlain Sidi Salem (Tortonian - Serravallian) was dated at 7.4Ma (EREX, 2012 after Rio, et. al., 1990). The base Messinian unconformity was believed to be a major regressive cycle followed by a transgression regime (7.4Ma to 6.6Ma) that was equivalent to NN11b zone (Figs. 5 and 6), (Rio, et. al., op. cit.). The sea level cycle shows that the (Lower Messinian) Qawasim Formation in El Basant field was deposited during the back filling of the previously formed incision. The back-fill is an interaction between the pure fluvial and marine depositional environments.

The regional seismic line interpretation indicates that the Lower Messinian (Qawasim Formation) in El Basant field is divided into two main levels, Qawasim level I and Qawasim level II. This regional seismic line shows the multi incisions phenomena of the Messinian sequence (Fig. 11). El Basant field is located at the periphery of a regional incision passing through the lower Messinian sequence (Qawasim Level I and Level II). This incision was re-incised with a younger incision during deposition Abu Madi Formation (Upper Messinian).

The Qawasim Level I sequence is considered as a channeling system at the base of the Lower Messinian incision. These channels show a low sinuosity nature clearly on the seismic RMS amplitude extraction (Fig. 12).

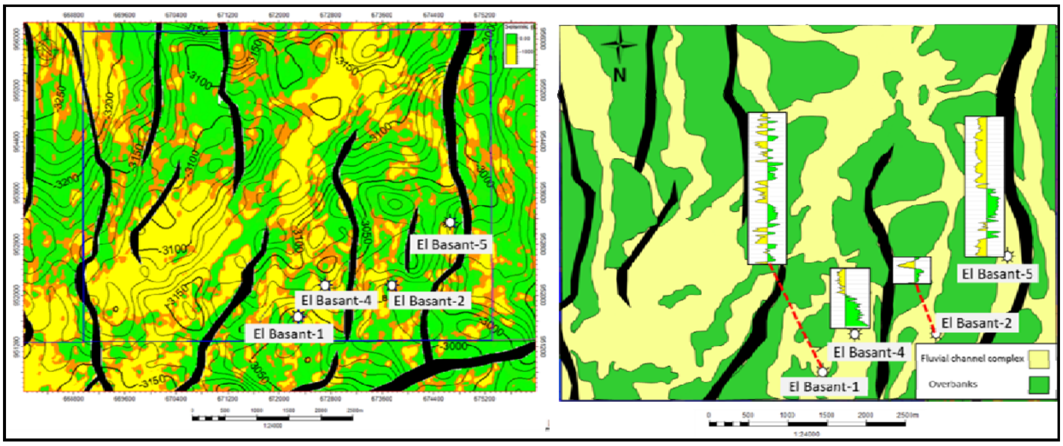

Fig. 12: (A) Depth structure contour map superimposed on full stack seismic amplitude (maximum negative), (B) Depositional element distribution of Qawasim Level I depending on the extracted seismic amplitude showing the N-NE general trend of the geobodies (fluvial channels) with the Gamma Ray log signature.

Depending on the facies associations of Qawasim Level I, this level may be a low sinuosity fluvial channels that overlaid the previously deposited braided channels in the depocenter of the incision to the west of El Basant field (Wasco, 2016 IR), (Figs. 12 and 14 Stage 1). The low sinuosity channels (Fig. 9) show a clear fining upward pattern, but in some parts they appeared as a coarsening upward pattern (ex. El Basant-1 and El Basant-5) that interpretation is based on:

The presence of crevasse splay channels complex.

The interference and transition of the regime from pure fluvial to fluvial-tidal regime which resulted in the formation of tidal-fluvial bars complex.

On the other hand, during the deposition of the Qawasim level II, the transgression started to be the dominant regime according to the sea level cycles of Rio et. al. 1990 (Figs. 5 and 6). This transgression turned the system to be an estuarine filling regime with tidal currents influx (Fig. 14 stage-2). This tidal influx affected Qawasim level II facies associations and formed estuarine tidal bars and channels deposits. The RMS seismic amplitude extraction shows the N-NE trends of the estuarine deposits (tidal bars and tidal channels complex) (Fig. 13).

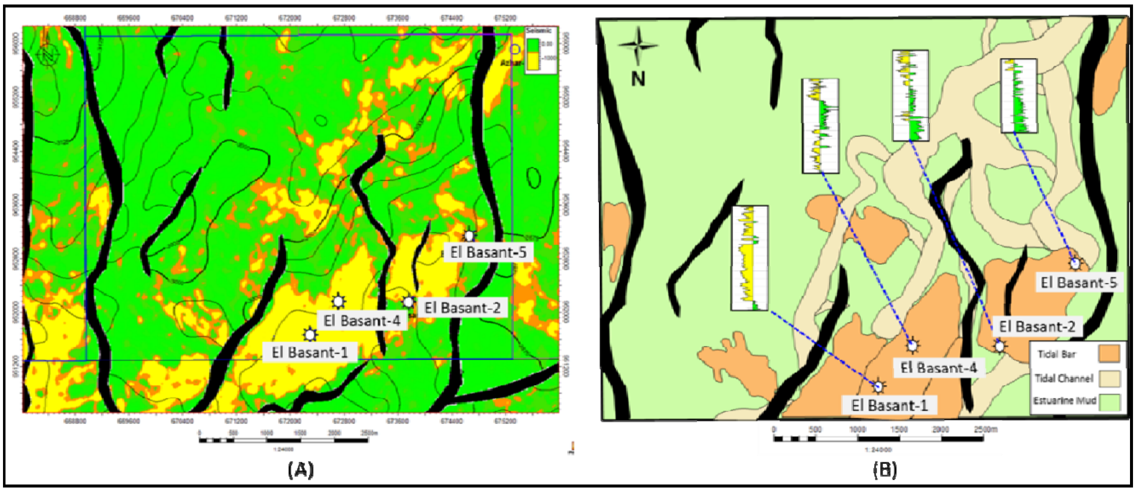

Fig. 13: (A) Depth structure contour map superimposed on full stack seismic amplitude (maximum negative), (B) Depositional element distribution of Qawasim Level II depending on the extracted seismic amplitude showing the NE general trend of the geobodies with the Gamma Ray log signature.

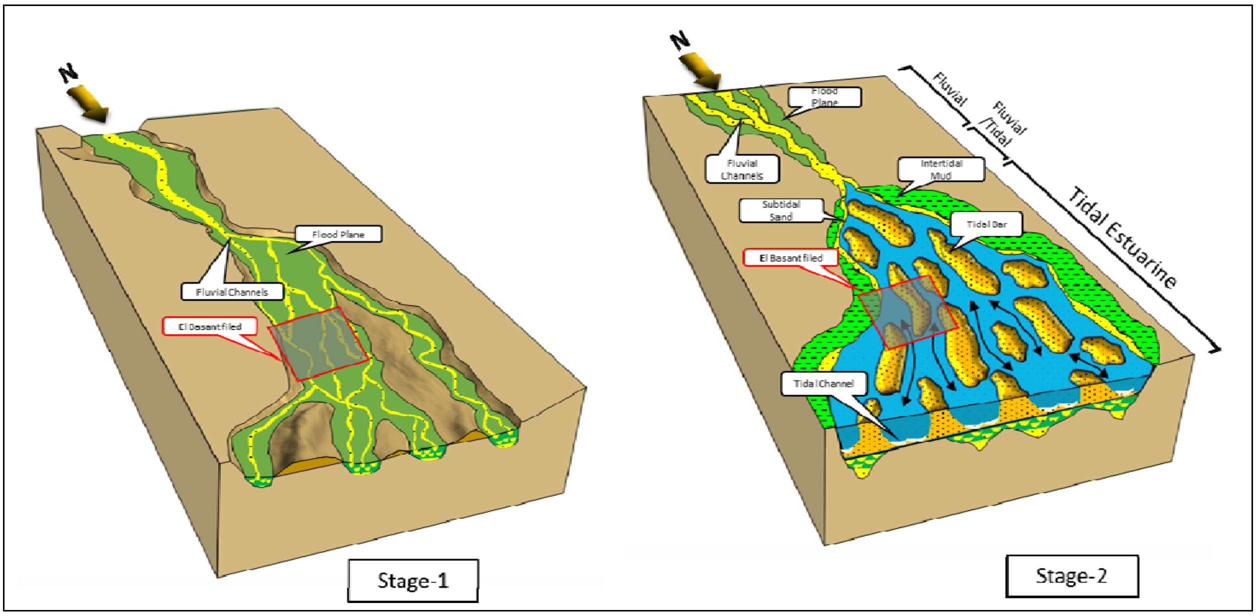

Fig. 14: Geological block diagram for the Proposed depositional model of El Basant area Stage-1: showing the fluvial channeling pattern at the base of Qawasim level I. Stage-2: showing the tide dominated estuarine facies distribution for Qawasim level II

REFERENCES

Abd El-Motaal and Kusky, (2003): Tectonic evolution of the intraplate s-shaped Syrian Arc foldthrust belt of the Middle East region in the context of plate tectonics. The 3rd Inter. Conf. geol. Afr., 2, 139-157.

Abd-Allah, A. M. A, Abdel Aal, M. H., and Ghandour, A., (2012): Structural characteristics and tectonic evolution of the northwestern margin of the Nile Delta, Egypt. J. Afri. Earth Sci.,68, 82-95.

Abd-Allah, A. M. A., (2008): Mesozoic-Cenozoic inversion tectonic of North Sinai: integration of structural and basin analysis. J. Appl. Geophys.,7, 77–108.

Abdel Aal, A., Price R. J., Vaitl J. D., Shrallow J. A., (1994): Tectonic evaluation of the Nile Delta, its impact on sedimentation and hydrocarbon potential, Egyptian Geological Petroleum Company 12th Exploration and Production Conference, 1, 19-34.

Abu El-Ella, R., (1990): The Neogene-Quatemary section in the Nile Delta, Egypt; geology and hydrocarbon potential. J.Petroleum Geol., 13, 329-340.

Ambrose, W. A., E. R. Ferrer, S. P. Dutton, F. P. Wang, A.Padron, W. Carrasquel, J. S. Yeh, and N. Tyler, (1995): Production optimization of tide-dominated deltaic reservoirs of the lower Misoa Formation (lower Eocene), LL-652 Area, Lagunillas field, Lake Maracaibo, Venezuela: The University of Texas at Austin, Bureau of Economic Geology Report of Investigations no. 226, 46.

Ayyad, M.H. and M. Darwish, (1996): Syrian Arc structures: a unifying model of inverted basins and hydrocarbon occurrences in North Egypt. Egyptian Geological Petroleum Company Seminar, November 1996, Cairo, 19.

Bosworth, W.; Guiraud, R. and Kessler, L. G., (1999): Late Cretaceous (~84 Ma) compressive deformation of the stable platform of NE Africa (Egypt): Far field stress effects of the 'Santonian event' and origin of the Syrian arc deformation belt. Geology, 27 (7), p. 633-636.

Carneiro de Castro, J., (1983): Facies, reservoirs and strati-graphic framework of the Mossoro Member (latest Cenomanian– earliest Turonian) in Potiguar Basin, NE Brazil: An example of a tide and wave dominated delta, in E. G. Rhodes and T. F. Moslow, eds., Marine clastic reservoirs: Examples and analogues: London, Springer-Verlag, 161 –182.

Dalrymple, R. W., and R. N. Rhodes, (1995): Estuarine dune sand bars, in G. M. E. Perillo, ed., Geomorphology and sedimentology of estuaries: New York, Elsevier Science, p. 359 –422.

Dixon, J.E., Clague, D.A., Wallace, P., and Poreda, R., 1997. Volatiles in alkalic basalts from the North Arch Volcanic Field, Hawaii: Extensive degassing of deep submarine-erupted alkalic series lavas. Journal of Petrology, in press

Dolson, J.C., A. El Barkooky, F. Wehr, P. D. Gingerich, N. Procharza, and M. Shann, (2002): The

Eocene and Oligocene Palaeo-geography of Whale Valley and the Fayoum basins: Implications for Hydrocarbon Exploration in the Nile Delta and Eco-Tourism, in the Greater Fayoum basin, Cairo, Egypt 2002: AAPG/EPEX/SEG/EGS/EAGE Field Trip No. 7

Dolson, J.C., Boucher, P.J., Siok, J., Heppard, P. D., (2005): Key challenges to realizing full potential in an emerging giant gas province. Nile Delta/Mediterranean offshore, deep water, Egypt. Petrol. Geol. Conf. series 6, p. 607–624.

Dolson, J. C., Shann, M. V., Matbouly, S. I., Hammouda, H., Rashed, R. M., (2001): Egypt in the twenty first century: petroleum potential in offshore trends. GeoArabia 6, p. 211-230.

Donselaar, M. E., and Schmidt, J. M., (2005): Integration of outcrop and borehole image logs for high-resolution facies interpretation: example from a fluvial fan in the Ebro Basin, Spain: Sedimentology, v. 52, no. 5, p. 1021 -1042.

EGPC, (1994): Nile Delta and North Sinai: Field discoveries and hydrocarbon potentials (A comprehensive overview). Egyptian General Petroleum Corporation, Cairo, Egypt, 387 p.

EREX, 2012): Biostratigraphic analysis of Balsam-1 well (Internal Reports).

Harms, J. C. and Wray, J. L., (1990): Nile Delta. In: Said, R. ed., The Geology of Egypt. Balkema, Rotterdam, p. 329-344.

Higley, D. K., (1994): 3-D Fluid-flow model of the House Creek field, Powder River Basin, Wyoming: AAPG Bulletin, 78(13), p. 171.

Hilgen, F. J., Kuiper, K. F., Krijgsman, W., Snel, E., Van der Laan, E., (2007): Astronomicaltuning as the basis for high resolution chronostratigraphy: the intricate history of the Messinian salinity crisis. Stratigraphy 2007, 231–238

Hussein, I. M. and Abd-Allah, A. M. A., (2001): Tectonic evolution of the northeastern part of the African continental margin, Egypt. J. Afr. Earth Sci., 33, 49-68.

Krijgsman, W., Meijer, P. T., (2008): Depositional environments of the Mediterranean “Lower Evaporites” of the Messinian salinity crisis: constraints from quantitative analyses. Mar. Geol. 253, 73–81. doi:10.1016/j.margeo.2008.04.010.

Loutit, T., Allard, D., Dolson, J.C., Schruers, J. and Laura, S. (2001): A New View of Egypt’s Hydrocarbon Potential (abs.). Middle East and North Africa (MENA) conf., London.

Marjanac, T., Steel, R. J., (1997): Dunlin Group sequence stratigraphy in the northern North Sea: a model for Cook Sandstone deposition. AAPG Bulletin 81, 256–292.

Martinius, A. W., P. S. Ringrose, A. Ness, and R. Wen, (2000): Multi-scale characterization and modelling of hetero-lithic tidal systems, offshore mid-Norway, in P. Weimer, R. M. Slatt, J. Coleman, N. C. Rosen, H. Nelson, A. H. Bouma, M. J. Spyzen, and D. T. Lawrence, eds., Deepwater reservoirs of the world: Gulf Coast Section SEPM 20th Annual Bob F. Perkins Research Conference, CD publication

Martinius, A. W., Kaas, I., Næss, A., Helgesen, G., Kjærefjord, J. M., and Leith, D. A., (2001): Sedimentology of the heterolithic and tide-dominated Tilje Formation (Early Jurassic, Halten Terrace, offshore mid-Norway), in Martinsen, O. J., and Dreyer, T., eds., Sedimentary environments offshore Norway – Paleozoic to recent: Norwegian Petroleum Society (NPF), Sp. Publ 10, 103–144.

Miall, A.D., 1985): Architectural-element analysis: a new method of facies analysis applied to fluvial deposits. Earth Science Review 22, 261 – 308.

Miall, A.D., (1996): The Geology of Fluvial Deposits. Springer Verlag, Berlin. p. 581.

Montanari, A., Beaudoin, B., Chan, L.S., Coccioni, R., Deino, A., de Paolo, D.J., Emmanuel, L., Fornaciari, E., Kruge, M., Lundblad, S., Mozzato, C., Portier, E., Renard, M., Rio, D., Sandroni, P., and Stankiewicz, A., (1997): Integrated stratigraphy of the Middle and Upper Miocene pelagic sequence of the Cònero Riviera (Marche region, Italy), in Montanari, A.,Odin, G.S., and Coccioni, R., eds., Miocene stratigraphy: An integrated approach: Devel. Palaeontol. Stratigr., v. 15, p. 409-450.

Mosconi, A., Rebora, A., Venturino, G., Bocc, P. and Khalil, M.H., (1996): Egypt-Nile Delta and North Sinai Cenozoic tectonic evolutionary model: A proposal. Proceedings 13th Petroleum Exploration and Production Conference, Cairo, Egypt, The Egyptian General Petroleum Corporation, 1, p. 203-223.

Moustafa, A.R. and Khalil, M.H., (1989): North Sinai structures and tectonic evolution. M.E.R.C. Ain Shams University Earth Sciences Series, 3, 215-231.

Moustafa, A. R. and Khalil, M. H., (1990): Structural characteristics and tectonic evolution of north Sinai fold belts. In R. Said "Geology of Egypt". A. A. Balkema, Rotterd Brookfield, 381-389.

Moustafa, A. R. and Khalil, M. H., (1994): Rejuvenation of the Eastern Mediterranean passive continental margin in northern and central Sinai: new data from the Themed fault. Geological Magazine 131, p. 435–448.

Nichols, G., (2009): Sedimentology and Stratigraphy, 2nd ed. Wiley-Blackwell.

Orwig, E. R., (1982): Tectonic framework of northern Egypt and the eastern Mediterranean regime. EGPC 6th Exploration Seminar, Egypt, p. 20.

Patton, T. L., Moustafa, A. R., Nelson, R. A., and Abdine, A. S., (1994): Tectonic evolution and structural setting of the Suez rift. In: London, S. M. (Ed.), Interior Rift Basins. AAPG Memoir 58, p. 9-55.

Pigott, J. D., and M. I. Abdel-Fattah, (2014): Seismic stratigraphy of the Messinian Nile Delta coastal plain: Recognition of the fluvial Regressive Systems Tract and its potential for hydrocarbon exploration: Journal of African Earth Sciences, 95, 9-21.

Reineck, H. E. and Singh, I. B., (1980): Depositional sedimentary environments. 2nd edn. Berlin: Springer.

Rio, D., Fornaciari E. & Raffi I., (1990): Late Oligocene through early Pleistocene calcareous nannofossils from western equatorial Indian Ocean (Leg 115). Proc. ODP, Sci Res., 115, 175-235.

Roveri, M., Lugli, S., Manzi, V., Schreiber, B.C., (2008): The Messinian Sicilian stratigraphy revisited: new insights for the Messinian salinity crisis. Terra Nova 20, 483–488.

Ruggieri, G. and Sprovieri, R., (1976): Messinian salinity crisis and its paleogeographical implications. Palaeogeogr, Palaeoclimatol., Palaeoecol., 20, 13-21.

Said, R., (1981): The Geological evolution of the River Nile. Springer-Verlag, Berlin, p. 151.

Said, R., 1990): Cenozoic. In: Said, R. ed., The Geology of Egypt. Balkema, Rotterdam, 451 –486.

Shahar, J., (1994): The Syrian Arc system: an overview. Palaeogeography, Palaeoclimatology, Palaeoecology, 112, 125–142.

Smith, G. A., (1988): Sedimentology of proximal to distal volcaniclastics dispersed across an active foldbelt: Ellensberg Formation (late Miocene), central Washington. Sedimentology, 35, 953-977.

Turner, P., (1974): Marine calcarenites from the Ringerike Group (‘Stage’ 10) of soutrhern Norway. Norsek geol. Tidsskr. 54, 1-12.

Uba, C. E., Heubeck, C., Hulka, C., (2005): Facies analysis and basin architecture of the Neogene Subandean synorogenic wedge, southern Bolivia. Institut für Geologische Wissenschaften, Freie Universität Berlin, Germany, Malteserstrasse, 74-100.

Verdier, A. C., T. Oki, and A. Suardy, (1980): Geology of the Handil field (East Kalimantan- Indonesia), in M 30: Giant oil and gas fields of the decade 1968–1978: AAPG Sp. Publ., 399-421.

WASCO, (2016): Regional study of the Upper and Lower Messinain sequence on El Wastani Petroleum company (WASCO) development leases (Internal Reports).

White, C. D., and M. D. Barton, (1999): Translating out-crop data to flow models, with applications to the Ferron Sandstone: Society of Petroleum Engineers Reservoir Evaluation & Engineering, 2(4), 18.

White, H. J., R. A. Skopec, F. A. Ramirez, J. A. Rodas, and G. Bonilla, (1995): Reservoir characterization of the Hollin and Napo formations, Western Oriente Basin, Equador, in A. J. Tankard, R. Suarez S., and H. J. Welsink, eds., Petroleum basins of South America: AAPG Memoir 62, 573 –596.

Wightman, D. M. and Pemberton, S. G., (1997): The Lower Cretaceous (Aptian) McMurray Formation: an overview of the Fort McMurray area, northeastern Alberta. In, Pemberton, S. G. and James, D. P., (eds.), Petroleum Geology of the Cretaceous Mannville Group, Western Canada, CSPG Memoir 18, 312-344.